Silva Gabreta	vol. 24	p. 69–84	Vimperk, 2018

Simulation of meteorological conditions in the Bohemian Forest

Beate Klöcking

Bureau of Applied Hydrology, Murnauer Str. 102a, D-81379 München, Germany
kloecking@bah-muenchen.de

Abstract
Knowledge of the meteorological conditions is essential for many applications, among those also for many research fields. Here, a reliable meteorological database for the extended area of the Bohemian Forest was developed. Meteorological data from 211 observation points were collected over a time span of 35 years. These data served as the basis for the simulation of climate conditions in the 4500 km^2 sized area with a spatial resolution of 100×100 m^2, as well as for the individual research plots of the "Silva Gabreta Monitoring" project. The simulation was performed using the geostatistical interpolation techniques included in the catchment model ArcEGMO.

Keywords: meteorological data, climate regionalisation, Bavarian Forest, Šumava

Introduction

Knowledge of the meteorological conditions at individual plots or spatially distributed over the whole area is essential for many research projects in the Bohemian Forest. Meteorological parameters have been monitored at individual sites, and by different institutions. Therefore, the quantity and quality of the different data series differ from site to site. Thus, the problem for any more sophisticated study such as the "Silva Gabreta Monitoring" projects was to get a reliable and consistent spatial distribution of the meteorological conditions over the whole study area from these station-based data. The specific topographic conditions of this low mountain lead to a huge heterogeneity, especially in air temperature and wind velocity even at the smallest scale. A further problem is the location of the Bohemian Forest at the border of three European countries, namely Austria, Germany and the Czech Republic, which implies that the concentration of meteorological observation sites is very sparse. Commercial products in the necessary spatial and temporal resolution are not available for all weather elements and the whole area until now. The German Weather Service (DWD), for example, offers regionalised daily precipitation data at a spatial resolution of 1×1 km^2 for the area of the German states only (DWD 2017). The HYRAS-dataset (Rauthe et al. 2013, Frick et al. 2014) covers Germany and the bordering river catchments, but only lasts from 1951 to 2006 and includes only gridded (5×5 km^2) datasets of air temperature and relative humidity as daily mean values besides the precipitation data.

The aim of the "Silva Gabreta Monitoring" projects is the allocation of biodiversity patterns in the Bohemian Forest. The climate database presented here will be used in combination with the collected species data (Frieß et al. 2018) to evaluate and predict ecological shifts induced by climate changes and potential consequences for the whole ecosystem.

The existing observational series of air temperature at 2 m above ground level, precipitation, global radiation, relative air humidity, and wind velocity from the different meteorological stations were collected and revised for the period 1980–2015. These station-based time series were then used as the underlying database for the calculation of the main meteorological parameters at the needed spatial and temporal resolution, namely daily values for each monitoring plot and yearly values at a spatial resolution of 100×100 m^2 for the whole study area.

Materials and methods

Study area

The study area covers about 4500 km^2 from the Danube River in the south to Sušice in the north with most of the Bohemian Forest (Šumava in Czech) (Fig. 1). It includes the Bavarian Forest National Park (240 km^2) in Germany and the western part of the Šumava National Park (690 km^2) in the Czech Republic. Altitudes range from 300 to 1450 m a.s.l. The mountain ridge, which extends from the Großer Osser Mt. in the north to the Dreisessel Mt. in the south, passing the Großer Arber, Großer Rachel and Lusen mounts, is nearly identical with

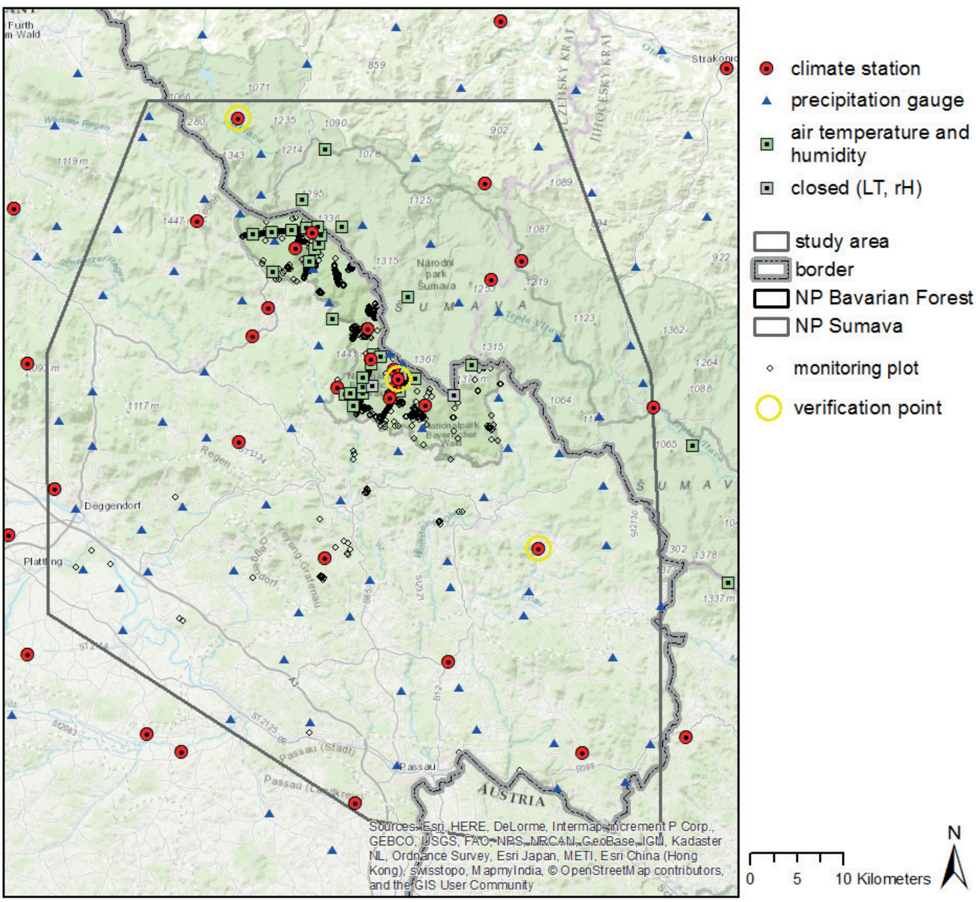

Fig. 1. Study area with meteorological stations and monitoring plots.

Table 1. Used meteorological observation sites with operator and type of data (ICS – incomplete climate station, e.g. only air temperature and humidity).

Company / Institution	Country	Number of observation sites		
		Climate	Precipitation	ICS
German Meteorological Service (DWD)	Germany	12	69	
Gewässerkundlicher Dienst Bayern (GKD, LfU)	Germany		7	
Landesamt für Umwelt, Referat Grundwasser monitoring (LfU)	Germany		1	
Agrarmeteorologischer Dienst Bayern (AMD)	Germany	8		
Institut für Meteorologie und Klimaforschung – Institut für atmosphärische Umweltforschung (IMK-IFU)	Germany	1		
Administration of the Bavarian Forest NP (NPV)	Germany	5		27
Landesanstalt für Wald und Forstwirtschaft (LWF)	Germany	2	3 (+36)	
WWA Deggendorf	Germany			1
Zentralanstalt für Meteorologie und Geodynamik Österreich	Austria	1		
Czech Hydrometeorological Institute (CHMI)	Czech Republic	9	23	
Administration of the Šumava NP	Czech Republic			6
Total	**211**	**37**	**139**	**35**

the border between Germany and the Czech Republic. It forms the central European divide of the Danube and Elbe rivers and represents a climatic border.

Characteristic for this area is its boundary position within the planetary circulation belt of the prevailing westerlies and continental influences from the east. The north-south orientation of the low mountain ranges additionally strengthens this climatic border. Relief-related microclimatic features are important – these include, among others, windward/leeward effects, which affect the distribution of precipitation, and cold-air accumulation in the valleys (Noack 1979, Elling 1987). The average annual precipitation total is between 800 mm in the lowlands and 1800 mm in the higher regions. The mean annual air temperature ranges between 3.0°C at high elevations and 9.9°C at low elevations (1980–2015).

Meteorological observational data

The first step was the collection of the available meteorological data series inside and in the vicinity of the study area. Table 1gives an overview of the number of used measuring stations and their origin (see Fig. 1).

The data were retrieved from the different providers, checked, and brought into the required format for the modelling. Depending on the origin of the data, it was also necessary to aggregate temporally higher-resolution data or disaggregate temporally lower-resolution (for example totalizers) data into the required time increment of one day. These changes mainly concerned the data of the administration of the Bavarian Forest National Park (NPV), the LWF and the IMK-IFU.

Besides its five meteorological stations (Waldhäuser, Schachtenau, Waldschmidthaus, Rachel- and Schachtendiensthütte), the NPV operates some sites where air temperature and humidity are measured for different research projects (listed in the last column of Table 1). Among them are 17 BIOKLIM stations (Bässler et al. 2015) with continuous measurements since 2006, and four (until 2007 five) sites on former windthrow areas with only summer measurements since 1987/1988. The monthly precipitation sums at seven BIOKLIM stations (also only in summer) and four windthrow-stations were disaggregated by adjacent reference stations to daily values. Prerequisite for this was the existence of a quasi-continuous precipitation reference time series in daily resolution from a nearby station.

The wind speed is measured at a limited number of sites only (cf. Figs. 2, 7). These data, measured at different heights above ground level, were transformed to equivalent 2 m-values as input for the calculation of the grass reference evapotranspiration (DVWK 1996, ATV-DVWK 2002) as follows:

$$v_2 = v_z \cdot \left(\frac{2}{z}\right)^a \quad (1)$$

where v_2 is wind speed at 2 m above ground level, v_z is wind speed at z m above ground level, and a is parameter in dependence of the surface roughness (0.13–0.7).

When evaluating the simulation results, it should be noted that, only at a few sites, there are continuous series of measurements of all required weather characteristics for the simulation period of 1 January 1980 to 31 December 2015 (see Fig. 2 for an overview of the available time series over the whole period). All measuring stations with time series of more than 180 daily values per year are counted as operational for the specific meteorological element in the year.

According to the fraction of the operational stations, the treated period can be sub-divided into three parts: 1980–1990 with a very poor meteorological database, 1991–2005 with improved coverage, and since 2006 with further continuous improvement of the database (air temperature and humidity, wind speed, and global radiation) especially by the setup of new (though mostly incomplete) climate stations in both national parks. The situation with regard to the precipitation measurements differs from this general trend, due to dismantling of many gauges by the DWD, which could only partly be compensated by the setup of new measurement sites by other providers. The particularly high fraction of precipitation gauges in the first period was caused by a measurement campaign of the summer precipitation in the research catchment Große Ohe (Thums 1993).

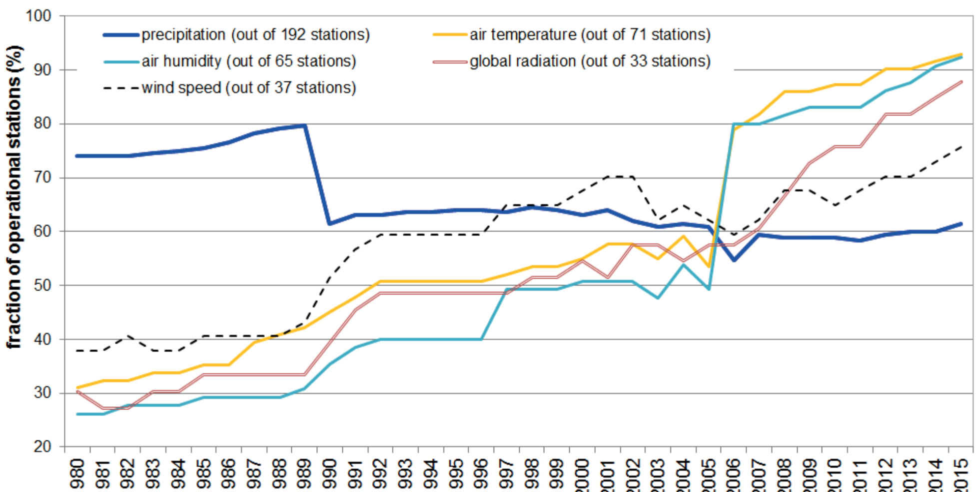

Fig. 2. Fraction of operational stations measuring precipitation (normalized to a total number of 192 stations), air temperature (normalized to 71 stations), air humidity (65 stations), global radiation (33 stations) and wind speed (37 stations).

Besides the temporal availability, the spatial distribution of the measuring stations is a crucial aspect for the regionalisation of its meteorological data. The correct position determination of the stations over the entire simulation period was difficult because of relocation, dismantling, and new setup of some observing stations. This particularly concerns the stations of the DWD. Overall, we found a high density in the central part of the Bavarian Forest National Park in the research catchment Große Ohe (Beudert et al. 2007) and around the Großer Falkenstein Mt. as a focus area of the BIOKLIM project since 2006 (Bässler et al. 2015). In the other parts of the study area, the number of measuring sites is scarce (see Figs. 4–8 for the individual meteorological elements).

Gaps in the time series were filled based on the readings of adjacent stations, employing the same technique as used for the regionalisation of the meteorological station based data (see model chapter). In doing so, the vertical and horizontal distances between the stations were taken into account, while windward/leeward effects were neglected.

GIS-model for the regionalisation of the meteorological data

In this study, two space models were built up to regionalise the station based data series, a grid-based model (100×100 m^2) for the whole study area and a point model including all monitoring plots.

An important prerequisite for the successful application of the regionalisation procedure is a good topographical characterisation of the study area. Since no high-resolution digital terrain model (DTM) was available for the Czech parts of the model area at the beginning of the project, the SRTM elevation model for Europe with a resolution of 90 m was used for these regions. This virtually free-to-air DTM was created in a joint effort by the National Aeronautics and Space Administration (NASA), The National Geospatial-Intelligence Agency (NGA), and German and Italian space agencies (Farr & Kobrick 2000). The characterisation of the German territories and all monitoring areas is based on the DTM5 of the Bavarian State Office for Digitization, Broadband and Surveying.

Model

The calculations were made with the geostatistical interpolation techniques included in the catchment model ArcEGMO (Becker et al. 2002 and Pfützner 2003). This model is a GIS-based, multi-scale modelling system for spatially simulating hydrological processes in river catchments, which has been adopted as the standard method for hydrological impact studies in the area of the Bavarian Forest National Park (Beudert et al. 2007).

The internal geostatistical interpolation techniques for regionalisation of meteorological input, the "Quadrant Method" and the "Inverse Distance Weighting Method" (nearest neighbour method), were primarily developed for application in mesoscale hydrological models. Consequently, they operate rapidly and use commonly available meteorological data (e.g. from the DWD). Although a relatively dense sampling network exists for precipitation in Germany, the other main measured values are recorded only at major meteorological stations. To allow for the effects of different spatial resolution for the individual weather values, a distinction is made between the regionalisation of data for point measurements of precipitation (total volume measured by precipitation stations and meteorological stations) and climate sampling (only meteorological stations). Series of measurements of precipitation, air temperature, wind speed, air humidity, as well as global radiation or duration of sunshine are expected for the climate sampling points.

In the "Inverse Distance Weighting Method", a variable number n of climate measurement points closest to the plot under consideration is used, independent of their direction concerning the plot. The „Quadrant Method" is based on values for the one station nearest to the

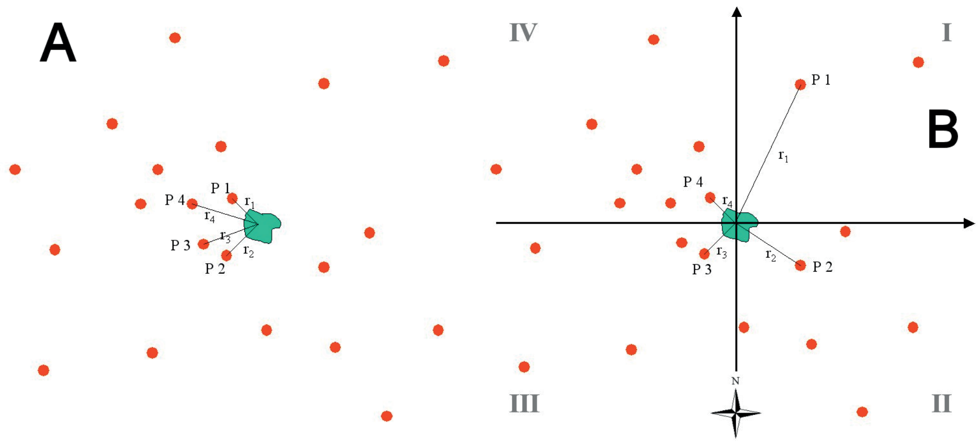

Fig. 3. Spatial distribution of selected measurement points around a sampling plot for the "Inverse Distance Weighting Method" with n = 4 (A) and the "Quadrant Method" (B).

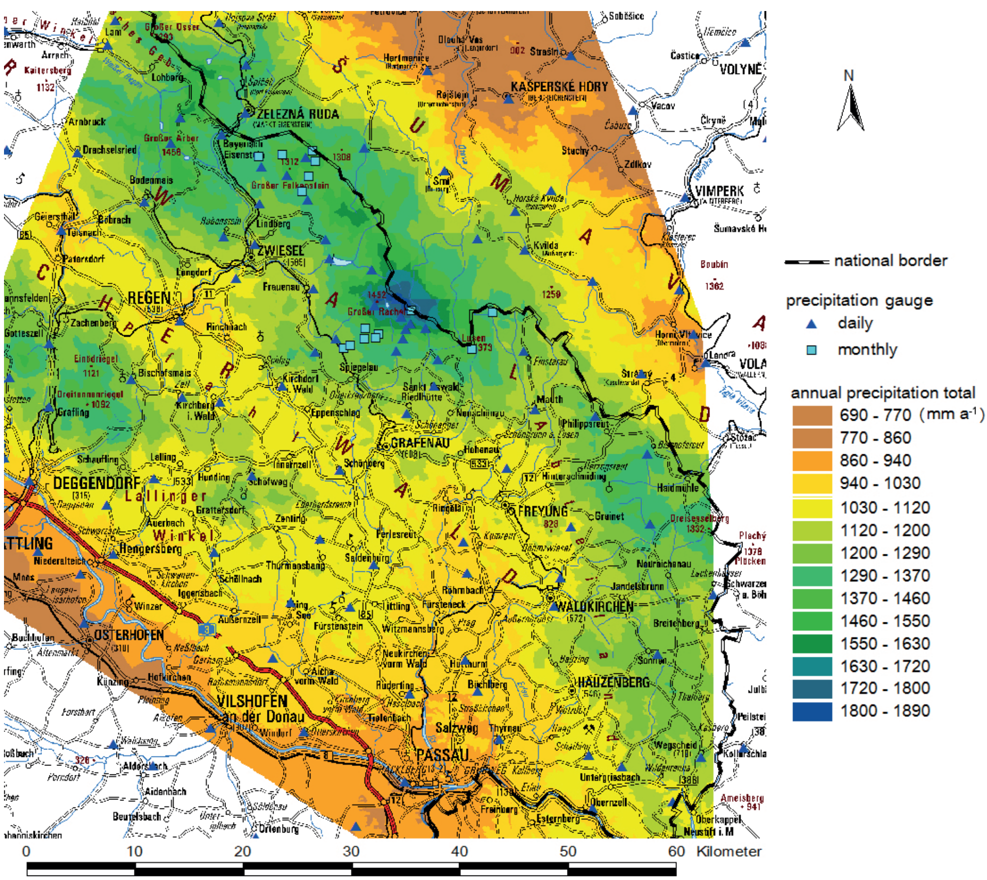

Fig. 4. Average annual precipitation total (mm) in 1980–2015.

centre in each quadrant (Fig. 3B). Thus, stations from all four directions are involved, which the "Inverse Distance Weighting Method" does not always guarantee (Fig. 3A).

Both methods employ vertical and horizontal distances between station and plot. Windward/leeward effects were neglected. The meteorological values P measured at n stations are weighted by distance according to equation 2 and allocated to the area of the plot. The sum of all weighting factors *g* is one.

$$P = \sum_{i=1}^{n} g_i P_i \qquad (2)$$

with $\sum_i g_i = 1$.

It should be emphasized that considerable problems can be caused by a low density of meteorological stations and longer gaps in the datasets. This is particularly critical in the case of extreme precipitation events. Specific analyses of this problem have been performed in the Stepenitz Basin by LAHMER et al. (2000), using different interpolation methods: the quadrant method, two Kriging methods, and several versions of the 'nearest neighbour' method. The quadrant method generally provides results which are almost as good as the more time-consuming Kriging methods.

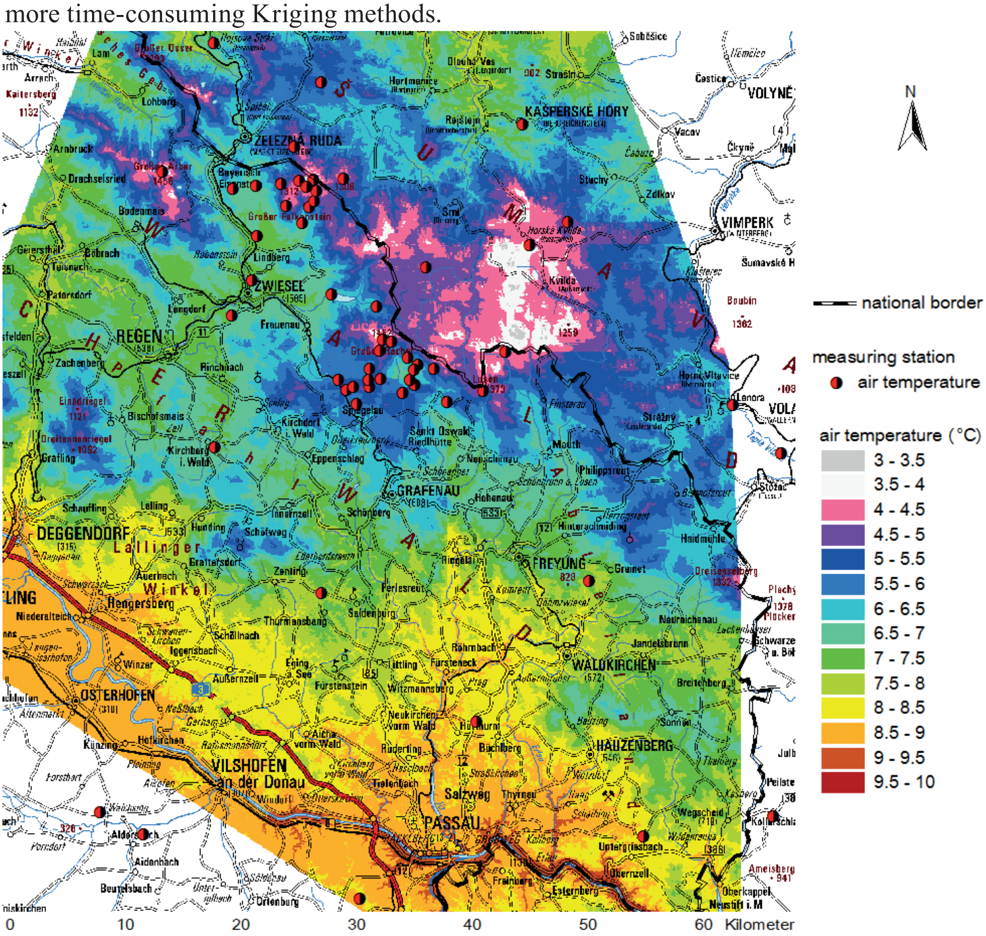

Fig. 5. Average annual air temperature (°C) in 1980–2015.

Allocation of values to the plots takes place under consideration of local topology. Therefore, the average dependence of the particular meteorological element *y* on altitude *h* is estimated by a linear regression ($y = a + b\ h$) using all daily measurements of that particular meteorological value in the simulation period. The Pearson correlation coefficient R is used as a measure of the linear correlation. It has a value between +1 and −1, where 1 is a total positive linear correlation, 0 is no linear correlation, and −1 is a total negative linear correlation.

$$R = \frac{\sum_{i=1}^{n}(h_i - \bar{h})(y_i - \bar{y})}{\sqrt{\sum_{i=1}^{n}(h_i - \bar{h})^2 \cdot \sum_{i=1}^{n}(y_i - \bar{y})^2}} \qquad (3)$$

with $\bar{h} = \frac{1}{n}\sum_{i=1}^{n} h_i$

and $\bar{y} = \frac{1}{n}\sum_{i=1}^{n} y_i$

Using this method, validated in many previous applications of ArcEGMO (e.g. Becker et al. 2002 and Pfützner 2013), we got the following average regression parameters (Table 2) for the period 1980–2015.

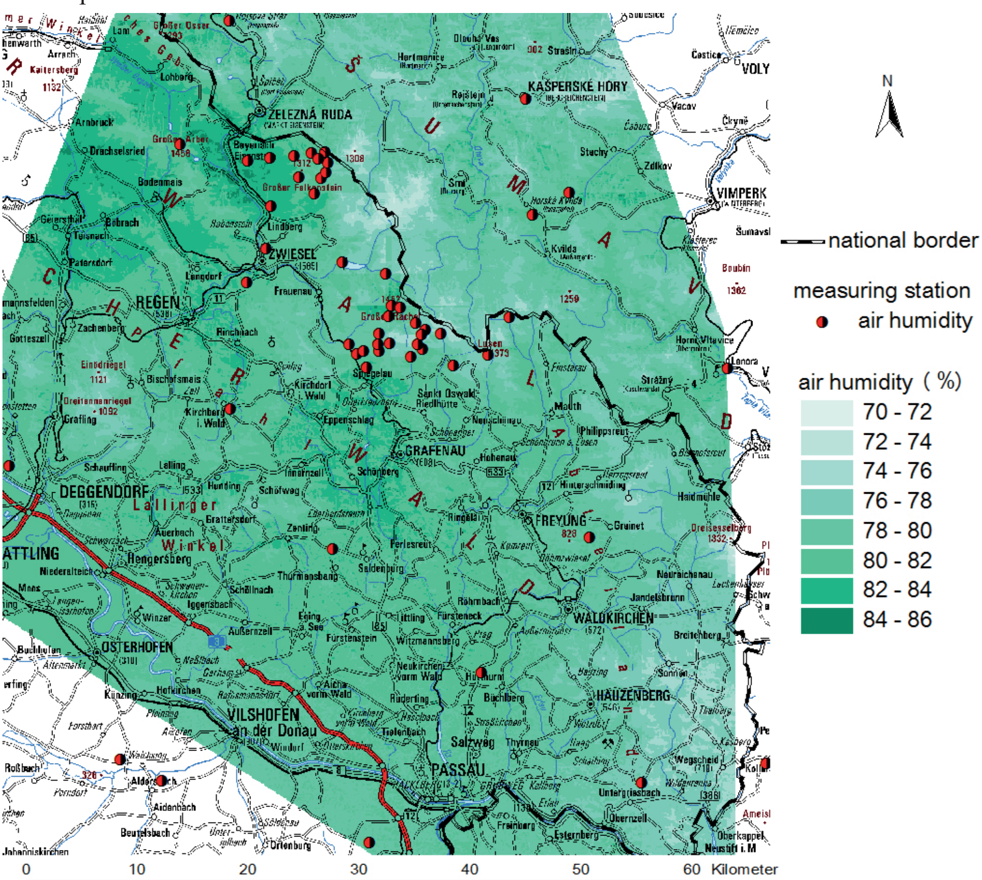

Fig. 6. Average annual air humidity (%) in 1980–2015.

Table 2. Regression and correlation coefficients for the altitude dependence of the different meteorological elements.

Attribute y	**elevation gradient** a **(m⁻¹)**	**regression coeff.** b	**Pearson coeff. R**
precipitation	0.0021	1.62	0.77
air temperature	−0.0046	10.05	–0.93
vapour pressure	–0.0028	10.62	–0.94
wind speed	0.0012	0.83	0.45

Despite different microclimatic conditions, there is a close correlation between altitude and precipitation, temperature, and vapour pressure. An exception is the calculated elevation gradient for the wind speed which does not match the expectations (see the low Pearson coefficient in Table 2).

The topology of a specific site influences global radiation and air temperature. To take this into account, we used the equivalent slope concept (Lee 1962) for calculating the slope and aspect dependent correction for the global radiation. The slope dependent modification of the temperature is done following Schulla (1997).

Locations with only short series of measurements (for example time series from specific temporary research projects) were excluded from the final regionalisation procedure. They

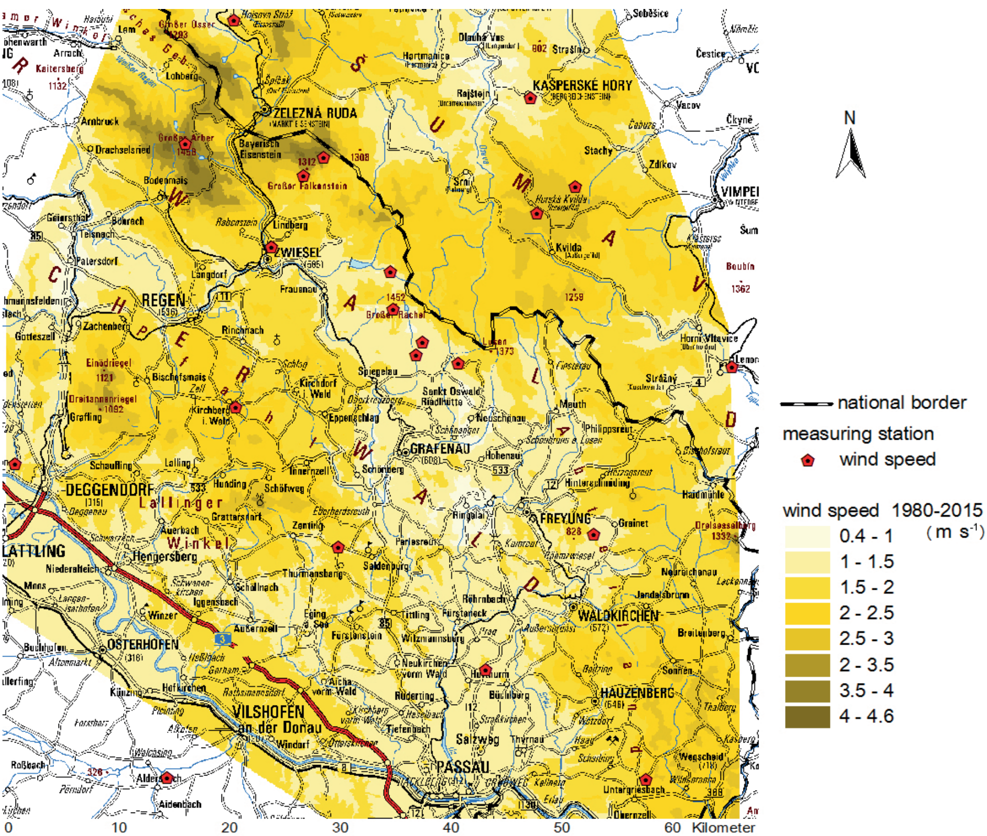

Fig. 7. Average annual wind speed 2 m above ground (m.s^{-1}) in 1980–2015.

were only used for gap filling and the calculation of the elevation gradients. The number of stations used as sampling points was thus reduced to 93 precipitation gauges and 71 complete and incomplete climate stations. Continuous time series of the included weather elements are thus available at all of these sampling points as truly observed or as interpolated values for 1 Jan 1980–31 Dec 2015. A correction of the precipitation (e.g. after Richter 1995) was not applied.

Results

The gridded spatial distribution of the main meteorological parameters was calculated by these 164 measuring stations using the Quadrant Method. The respecting figures show precipitation amounts (Fig. 4), air temperature (Fig. 5), air humidity (Fig. 6), wind speed (Fig. 7), and global radiation (Fig. 8) as arithmetic means of the simulated daily values for each grid in the period 1980–2015.

The specific yearly values for each of the 100×100 m² grid cells are available at the administration of the Bavarian Forest National Park (NPV). Data with a higher temporal resolution (day or month) can be provided for sections of the study area upon reasonable request. The meteorological parameters at the 1073 individual monitoring plots in the study area (Fig. 1) were calculated in daily, monthly and yearly resolution.

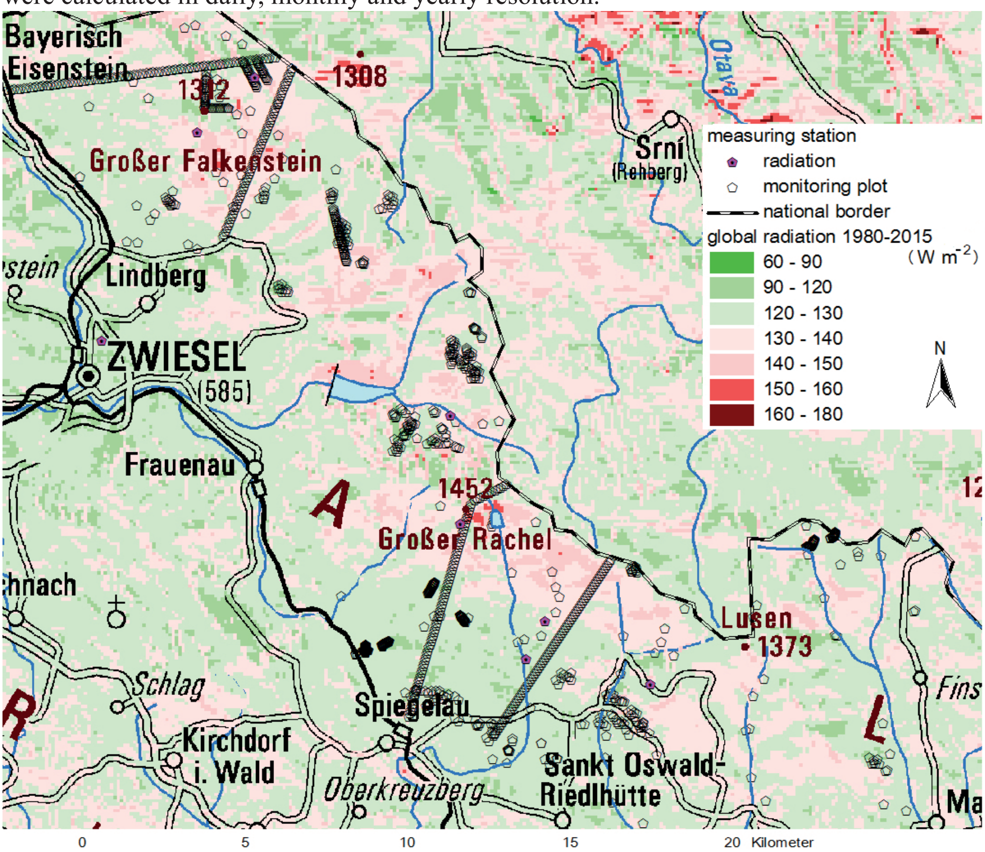

Fig. 8. Average annual global radiation (W.m^{-2}) in the central part of the Bohemian Forest (1980–2015).

Table 3. Comparison of interpolated and measured meteorological elements for three meteorological stations

Station / element	sample size	average value obs.	average value sim.	RMSE	NRM-SE	tole-rance (±)	fraction outside (%)
RDH (Rachel-Diensthütte)							
precipitation (mm.d^{-1})	12536	4.34	4.17	1.85	0.42	5	2.7
air temperature (°C)	3947	7.37	7.07	0.57	0.08	2	0.3
air humidity (%)	3814	79.6	79.3	3.54	0.04	10	1.1
Grainet-Rehberg							
precipitation (mm.d^{-1})	13119	3.03	3.14	1.87	0.62	5	2.9
air temperature (°C)	13119	7.64	7.38	0.90	0.12	2	3.4
air humidity (%)	13112	80.39	81.34	5.17	0.06	10	5.8
wind speed (m.s^{-1})	8401	1.60	0.92	0.91	0.57	2	5.9
global radiation (J.cm^{-2})	3954	1045	1068	74.34	0.07	200	39.5
Hojsova Stráž							
precipitation (mm.d^{-1})	13149	3.18	3.57	2.39	0.75	5	4.6
air temperature (°C)	9861	6.67	6.21	1.02	0.15	2	8.6
air humidity (%)	9861	80.12	81.98	6.16	0.08	10	13.1
wind speed (m.s^{-1})	9861	1.46	2.37	1.12	0.77	2	12.0
global radiation (J.cm^{-2})	3255	798	866	59.68	0.07	200	31.8

The reliability of these results is determined not only by the quality of the weather measurement series and station density, but also by the topological characteristics (ground level, slope and orientation) of the individual areas. These values were determined from the DTMs as a spatial average over the individual area. Location errors especially affect the quality of the radiation and temperature calculation. The assessment must, therefore, be carried out separately for each area and the individual time periods, taking into account these boundary conditions. Overall, the spatial distribution of the simulation results seems plausible for the entire period of 1980–2015 and was also double-checked for consistency against the Czech Climatological and German Hydrological Atlas (Tolasz et al. 2007, HAD 2013). The only exception is the spatial distribution of the wind conditions (Fig. 7). The simulated wind speed at the mountain ridge between the Rachel and Lusen mounts seems to be too low. Here, the simulation is based on the measured wind data of five (seven for gap filling) stations of the NPV. The mean wind speeds at 2 m, calculated from these time series, are significantly lower than for other stations at comparable altitude. The reasons for this (possible measurement errors, lee effects, specific topographic situation in the Große Ohe catchment, or others) remains to be determined.

Besides this plausibility check of the spatial distribution, the uncertainty of the interpolated time series has been analysed for different representative sites. Three sites were selected: one grid cell in the catchment Große Ohe including the climate station Rachel-Diensthütte (RDH) at 874 m a.s.l. as an example for an area with many surrounding measuring stations, and two grid cells with a low density of surrounding climate stations, namely the grid cell icluding the CHMI-climate station Hojsova Stráž (867 m a.s.l.) and the grid cell with the DWD climate station Grainet-Rehberg (628 m a.s.l.) (marked as verification points in Fig. 1).

The daily simulation results of two different model runs were compared for these three grid cells. The first simulation was done including the specific climate station. These results are labelled as "observed". In the second run, this station was excluded (labelled as "simulated" or "interpolated" values in the following). Only periods with existing measurements for the specific meteorological element were taken into account. Table 3 shows the sample size and the mean values for each evaluated element of the three sites. The Root Mean Square Error (*RMSE*, equation 4) and its normalised value *NRMSE* (equation 5) were used as criteria for the assessment of the reliability of the simulation results:

$$RMSE = \sqrt{\frac{\sum_{i=1}^{n}\left(y_i^{sim} - y_i^{m}\right)^2}{n}} \tag{4}$$

and $$NRMSE = \frac{RMSE}{\overline{y^m}} \tag{5}$$

with $\overline{y^m} = \frac{1}{n}\sum_{i=1}^{n} y_i^m$

where y^m is the observed value, y^{sim} is the simulated value and n the sample size.

We imposed an allowed tolerance range for each meteorological element from the viewpoint of hydrological modelling, based on the sensitivity of the model against this input value. This range is marked with red lines in all y^{sim}-y^m-plots (Figs. 9–13). For the regions with a high density of stations this range corresponds to the 3-RMSE-confidence interval.

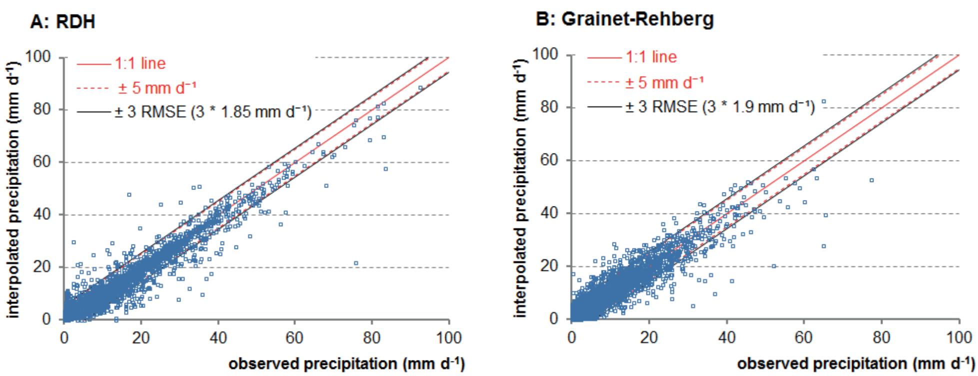

Fig. 9. Comparison of measured and interpolated values of daily precipitation sum at a site with a high station density (A: RDH) and a a site with a low station density (B: Grainet-Rehberg).

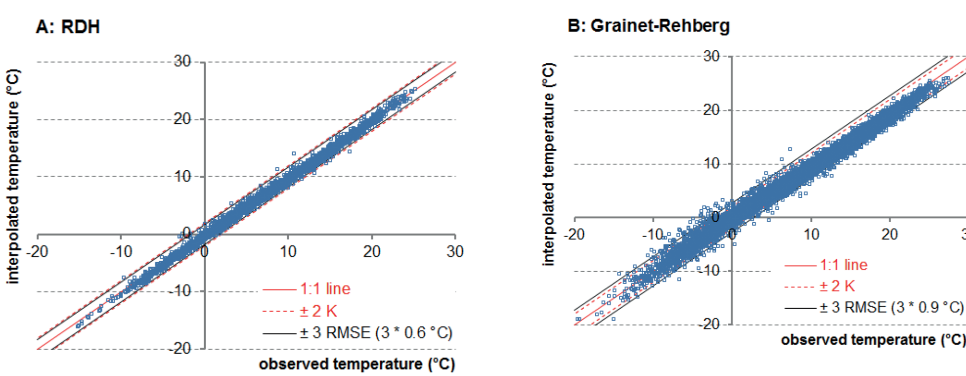

Fig. 10. Comparison of measured and interpolated values of daily air temperature at RDH (A) and Grainet--Rehberg (B).

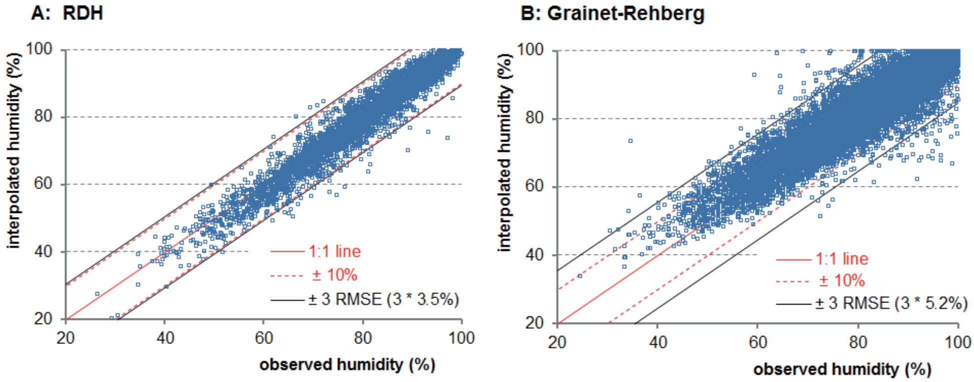

Fig. 11. Comparison of measured and interpolated values of daily air humidity at RDH (A) and Grainet--Rehberg (B).

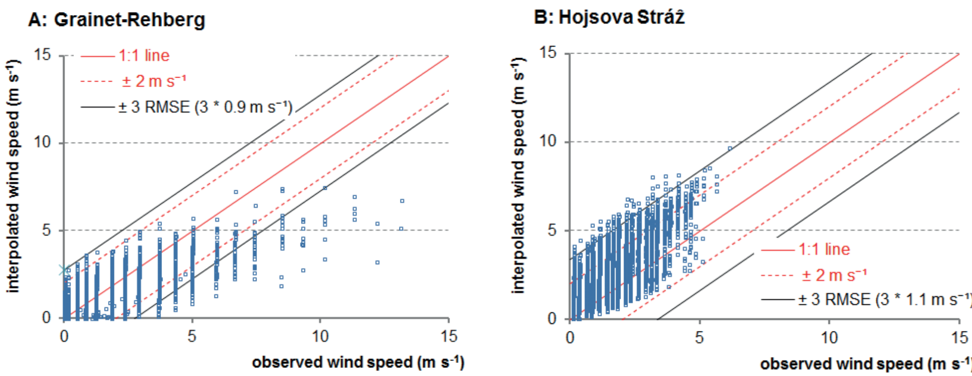

Fig. 12. Comparison of measured and interpolated values of daily wind speed at Grainet-Rehberg (A) and Hojsova Stráž (B).

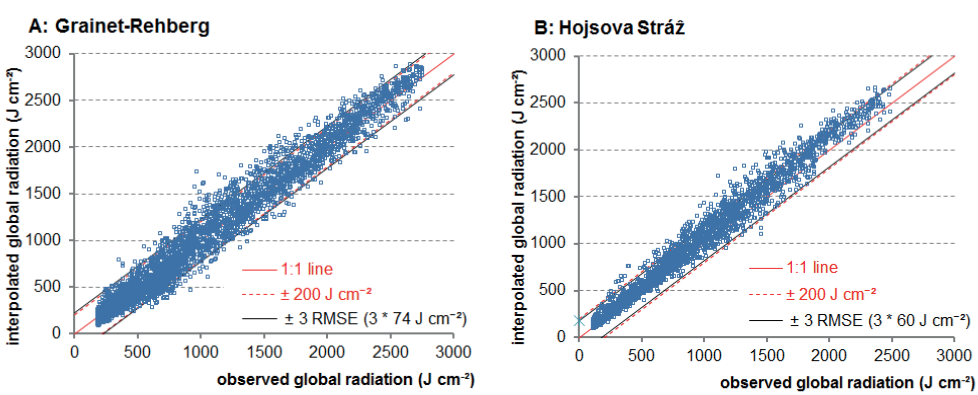

Fig. 13. Comparison of measured and interpolated values of daily global radiation at Grainet-Rehberg (A) and Hojsova Stráž (B).

The agreement between observed and interpolated values of temperature and global radiation is very good at all investigated sites. The simulated daily values fit the observed values over the whole period, as the low *NRMSE* (<0.2) show. The 3-*RMSE*-confidence intervals fall within the imposed range (Figs. 10, 13). Though the *NRMSE* for the precipitation values is significantly higher, the concordance of observation and interpolation is still acceptable. More than 95% of all interpolated daily precipitation values of the investigated sites are inside the tolerance range of ±5 mm.d^{-1} (Fig. 9, Table 3).

The positive impact of a high station density is clearly visible by direct comparison of the results for RDH and Grainet-Rehberg. The fraction of data points inside the tolerance frame is higher for RDH (Figs. 9–11), especially in case of the results for air humidity. Thougth the *NRMSE* for the humidity are very low at all sites, the interpolation results are not satisfying for Hojsova Stráž (not pictured but similar to the Grainet-Rehberg cell) and Grainet-Rehberg. The dispersion of the daily humidity values is critical (Fig. 11).

The results of the interpolation of the wind speed data are unsatisfactory too, as is shown by the high *NRMSE*-values (Table 3) and the distribution of data points (Fig. 12). The interpolated wind speed values are only reliable in the surrounding areas of the rare wind measuring stations.

As these figures demonstrate, the spatial density of surrounding stations directly determines the accuracy of the interpolation results. This translates into different reliability of the results in the three temporal intervals defined via the number of operational stations (Fig. 2). Thus, the results are less confident for the period of 1980–1990. The increasing number of measuring sites from 1991 until 2005 results in an improvement of the reliability. Since 2006, we have the maximum of operational stations, which raise the reliability further, especially for the central part of the Bavarian Forest National Park.

Conclusions

All known time series of meteorological data available in the surrounding area of the two national parks were collected, checked and, if necessary, cleaned up and put into a uniform format for the period 1980–2015. These daily time series are available for a total of 211 stations for further evaluation. These time series will be updated periodically, and extended in case of the newly set-up stations.

Based on these data, the present goal was to describe the meteorological conditions in this 4500 km^2 study area at a spatial resolution of 100×100 m^2. For this, the "Quadrant Method" was used, an internal geostatistical interpolation technique of the hydrological model ArcEGMO. The assessment of the reliability of the modelling results demonstrates its usability at large areas, with some restrictions (e.g. wind speed and air humidity). The quality of the results is very good for areas with a high station density, but decreases with a lower number of surrounding stations. Yet, the results for temperature, precipitation and radiation are still reliable for the regions with a low density of measuring stations.

This finding is consistent with the reliability estimates in previous hydrological modelling studies in the Ilz and the Große Ohe catchments (Klöcking et al. 2005, Beudert et al. 2007, Sprenger et al. 2013). The simulated stream discharges as an integrating element of the conditions in a catchment (including the meteorological characteristics) fit very well the observed values at all discharge gauges.

Despite the restrictions (e.g. wind, humidity), the results of this regionalisation method can be used for further research projects in this region, such as the allocation of biodiversity patterns in the "Silva Gabreta Monitoring" project.

If higher accuracy is required, new interpolation methods need to be developed, including small-scale weather phenomena, or windward/leeward effects. Testing and verification of these new methods can be done with the herein developed database.

Acknowledgements. This contribution was supported by the Cross-border cooperation programme Czech Republic–Bavaria Free State ETC goal 2014–2020, the Interreg V project No. 26 "Silva Gabreta Monitoring – Implementation of Transboundary Monitoring of Biodiversity and Water Regime".. I am grateful to the providers (see Table 1) of the observed time series.

References

ATV-DVWK, 2002: Verdunstung in Bezug zu Landnutzung, Bewuchs und Boden. *Merkblatt ATV-DVWK-M* 504, 144 pp.

Bässler C., Seifert L. & Müller J., 2015: The BIOKLIM Project in the National Park Bavarian Forest: Lessons from a biodiversity survey. *Silva Gabreta*, 21: 81–93.

Becker A., Klöcking B., Lahmer W. & Pfützner B., 2002: The hydrological modelling system ArcEGMO. In: *Mathematical models of large watershed hydrology*, Singh V.P. & Frevert D.K. (eds) Water Resources Publications, Littleton, Colorado: 321–384.

Beudert B., Klöcking B. & Schwarze R., 2007: Große Ohe: impact of bark beetle infestation on the water and matter budget of a forested catchment. In: *Forest Hydrology – results of research in Germany and Rusia, Part I*, Puhlmann H. & Schwarze R. (eds) IHP/HWRP-Berichte, Heft 6: 41–63.

DVWK, 1996: Ermittlung der Verdunstung von Land- und Wasserflächen. *DVWK Merkblätter zur Wasserwirtschaft* 238, 135 pp.

DWD, 2017: REGNIE (REGionalisierte NIEderschläge): Verfahrensbeschreibung und Nutzeranleitung. Ms., interner Bericht im DWD, Abteilung Hydrometeorologie, Offenbach, 9 pp.

Elling W., Bauer E., Klemm G. & Koch H., 1987: *Klima und Böden. Waldstandorte. Nationalpark Bayerischer Wald, Heft 1*. Schriftenreihe des Bayerischen Staatsministeriums für Ernährung, Landwirtschaft und Forsten, Grafenau, 255 pp.

Farr T.G. & Kobrick M., 2000: Shuttle Radar Topography Mission produces a wealth of data. *EOS Transactions of American Geophysical Union*, 81: 583–585.

Frick C., Steiner H., Mazurkiewicz A., Riediger U., Rauthe M., Reich T. & Gratzki A., 2014: Central European high-resolution gridded daily data sets (HYRAS): Mean temperature and relative humidity. *Meteorologische Zeitschrift*, 23/1: 15–32.

Friess N., Bässler C., Brandl R., Hilmers T., Müller J. & Seifert L., 2018: Biodiversity along an elevational gradient of the Bavarian Forest – The BIOKLIM project. *Silva Gabreta*, 24: 149–160.

HAD, 2013: *Hydrologischer Atlas von Deutschland*. Bundesministerium für Umwelt, Naturschutz und Reaktorsicherheit (BMU). Online http://geoportal.bafg.de/mapapps/resources/apps/HAD/index.html?lang=de

Lahmer W., Pfützner B. & Becker A., 2000: Data-related uncertainties in meso- and macroscale hydrological modelling. In: *Accuracy 2000. Proceedings of the 4th international symposium on spatial accuracy assessment in natural resources and environmental sciences*. Heuvelink, G.B.M. & Lemmens, M.J.P.M (eds). Amsterdam: 389–396.

Lee R., 1962: Theory of the "equivalent slope". *Monthly Weather Review*, 90: 165–166.

Noack E.M., 1979: *Witterung und Klima im Nationalpark Bayerischer Wald. Nationalpark Bayerischer Wald, Heft 5*. Schriftenreihe des Bayerischen Staatsministeriums für Ernährung, Landwirtschaft und Forsten, München, 132 pp.

Pfützner B. (ed.), 2003: *Modelldokumentation ArcEGMO*. Online http:\\www.arcegmo.de

Pfützner B., Klöcking B., Schumann A. & Hesse P., 2013: *Klimafolgenstudie 2012 – Wasser: Untersuchung zu den Folgen des Klimawandels in Sachsen-Anhalt*. Berichte des Landesamtes für Umweltschutz Sachsen-Anhalt, Heft 5 (Band 1), 176 pp.

Rauthe M., Steiner H., Riediger U., Mazurkiewicz A. & Gratzki A., 2013: A Central European precipitation climatology–Part I: Generation and validation of a high-resolution gridded daily data set (HYRAS). *Meteorologische Zeitschrift*, 22/3: 235–256.

Richter D., 1995: *Ergebnisse methodischer Untersuchungen zur Korrektur des systematischen Messfehlers des Hellmann-Niederschlagsmessers*. Berichte des Deutschen Wetterdienstes Nr. 194, Offenbach, 93 pp.

Schulla J., 1997: *Hydrologische Modellierung von Flussgebieten zur Abschätzung der Folgen von Klimaänderungen*. Zürcher Geographische Schriften 69, ETH Zürich, 161 pp.

Sprenger W., Blomenhofer A., Klöcking B., Neumann J. & Wendel S., 2013: *Fallstudie Ilz – Auswirkungen des Klimawandels auf den Grundwasserhaushalt und die Wasserversorgung im Bayerischen Wald*. KLIWA-

Berichte, Heft 19: 227–236.
Thums S., 1993: *Niederschlags- und Abflussauswertung der 10jährigen Messreihe 1980–1989 für das Einzugsgebiet der Großen Ohe. Wasserhaushalt und Stoffbilanzen im naturnahen Einzugsgebiet Große Ohe Bd. 5*. Nationalpark Bayerischer Wald, 196 pp.
Tolasz R. (ed.), 2007: *Climate Atlas of Czechia*. Czech Hydrometeorological Institute, Prague, 254 pp.

Received: 28 June 2018
Accepted: 4 November 2018